




Article

# Prediction of Wave Energy Transformation Capability in Isolated Islands by Using the Monte Carlo Method

Deivis Avila <sup>1,\*</sup> , Graciliano Nicolás Marichal <sup>1,\*</sup> , Ramón Quiza <sup>2,\*</sup>  and Felipe San Luis <sup>1,\*</sup>

<sup>1</sup> Higher Polytechnic School of Engineering (EPSI), University of La Laguna, 38001 Tenerife, Spain

<sup>2</sup> Centre for Advanced and Sustainable Manufacturing Studies, University of Matanzas, Autopista a Vardero km 3.5, Matanzas 44740, Cuba

\* Correspondence: [davilapr@ull.edu.es](mailto:davilapr@ull.edu.es) (D.A.); [nicomar@ull.edu.es](mailto:nicomar@ull.edu.es) (G.N.M.); [ramon.quiza@umcc.cu](mailto:ramon.quiza@umcc.cu) (R.Q.); [fsanluis@ull.edu.es](mailto:fsanluis@ull.edu.es) (F.S.L.)

**Abstract:** In this work, a mathematical computer simulation model is used to predict the possible energy generated from different Waves Energy Converters (WECs) in the Canary Islands. The Monte Carlo Method is the computer simulation model proposed to predict the generated energy. The Waves Energy Converter systems analyzed in the study were, the Aqua Buoy, Wave Dragon and Pelamis converters. The models were implemented and validated, with the dataset of Gran Canaria deep water buoy. This buoy belongs to a network of buoys belonging to Spain's State Ports and they cover a dataset period of 22 years. The research has concluded that it is possible to affirm that the achieved model is a strong tool to compute the possible energy of any WECs, when the power matrix is known. The model based on the Monte Carlo simulation can be used in isolated islands of the Atlantic Ocean and can be extrapolated to other regions with the same characteristics.

**Keywords:** wave energy; WECs; Monte Carlo method; Canary Islands



**Citation:** Avila, D.; Marichal, G.N.; Quiza, R.; San Luis, F. Prediction of Wave Energy Transformation Capability in Isolated Islands by Using the Monte Carlo Method. *J. Mar. Sci. Eng.* **2021**, *9*, 980. <https://doi.org/10.3390/jmse9090980>

Academic Editor: Silvio Barbarelli

Received: 28 July 2021

Accepted: 1 September 2021

Published: 7 September 2021

**Publisher's Note:** MDPI stays neutral with regard to jurisdictional claims in published maps and institutional affiliations.



**Copyright:** © 2021 by the authors. Licensee MDPI, Basel, Switzerland. This article is an open access article distributed under the terms and conditions of the Creative Commons Attribution (CC BY) license (<https://creativecommons.org/licenses/by/4.0/>).

## 1. Introduction

Spain has been a member of the European Union (EU) since January of 1986. The EU is an economic and political unification; currently there are 27 member states, including the UK, that are subject to the obligations and the privileges within the common judicial and legislative institutions. The EU recognize nine outermost regions, which are geographically far from the European continent. Only three countries (France, Portugal and Spain) have territory in the outermost regions, out of all the members of the EU [1,2]. These distant regions of Continental Europe represent a logistical challenge in many different fields, especially from an energy point of view. The energy production and transportation depend on imported fuels. In general, the electricity systems in the outermost regions are isolated. This fact increases the difficulty of its optimization [3–6].

The outermost regions in the North Atlantic Ocean are Azores and Madeira (Portugal). The Canary Islands (Spain) are the three Macaronesian archipelagos within the EU. All of them with volcanic origin and similar characteristics [7].

Figure 1 shows the Canary Islands that are formed by eight main volcanic islands located on the North Atlantic Ocean (27.5° N–29.5° N, 13° W–18.5° W), only 115 km away from the African continent. The population registered in the Canary archipelago at the end of 2019 was 2,153,389 inhabitants. Tourism is the economic driver of the Canary Islands. Every single year millions of tourists visit the islands, except in 2020 due to the COVID-19 pandemic. The climate on the islands is generally warm and dry, creating arid almost desert-like conditions on the eastern islands (Lanzarote and Fuerteventura). Due to all these weather conditions, the Canarian archipelago has a serious water scarcity problem. Therefore, the service sector industry is only conceivable through the desalination of seawater, although this water is also used in agriculture and in supplying the population [3,4,6–12]. Another difficulty in the archipelago is energy production. For the electrical network and

electricity transportation, more than the 95% of the energy consumption comes from importations of fuels, with its respective problem of environmental contamination. The depths of the adjacent seawater are too great around most of the eight Canarian islands, which prevents the laying of submarine electrical cables between all the islands and with the African Continent, except between Lanzarote and Fuerteventura and Tenerife and La Gomera. The energy needs must be supplied locally in the majority of the islands [3–6,13].

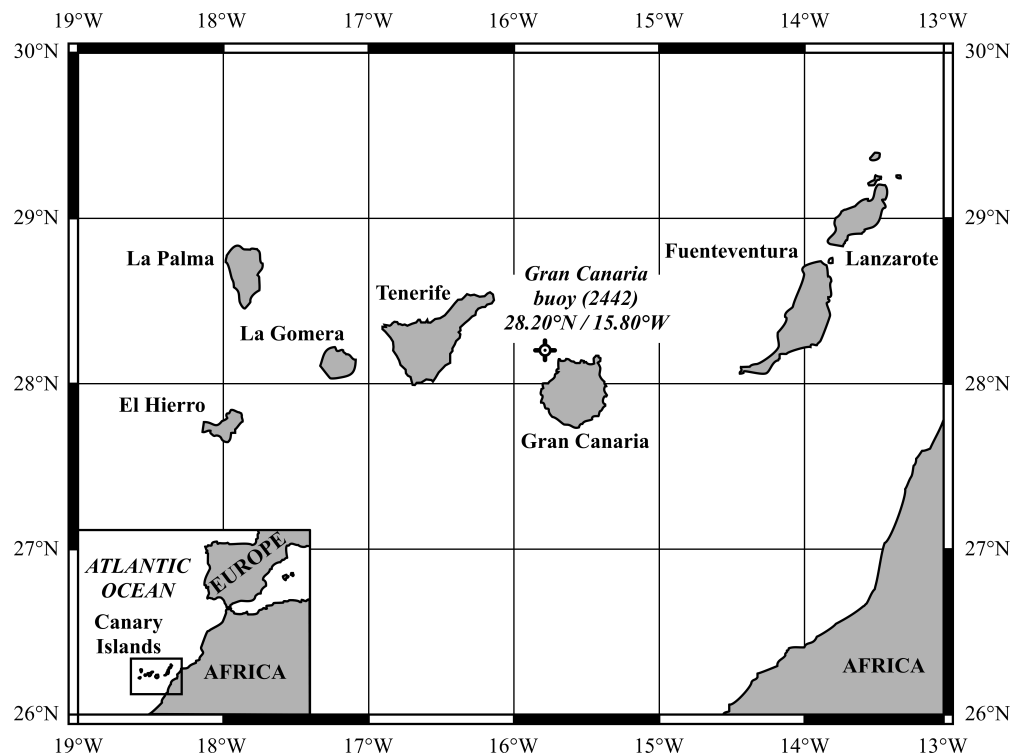


**Figure 1.** Gran Canaria buoy (2442) location.

For many decades the local government, in coordination with the Government of Spain, has sought an energy alternatives for remote islands. Due to this, it has focused a special interest on renewable energies (RE). Therefore, research and development institutions have been created to promote the use and generation of renewable energies. One example is the “Canary Islands Institute of Technology (ITC)” or “Gorona del Viento S.A.” ([www.goronadelviento.es](http://www.goronadelviento.es), accessed on 30 August 2021), on El Hierro Island. This last institution has as a main objective to supply 100% of electrical energy from a hybrid renewable energy system (Wind-Pumped Hydro Power Station) in this small island [14].

Due to the geographical situation of the Canary Islands, it has abundant renewable sources such as wind and solar, which are increasingly used for the generation of electricity. In spite of several efforts that have been done to promote different kinds of the renewable energies (RE), little attention has been focused on wave energy, although different studies have shown that there is a considerable wave resource (25–30 kW/m) on the north and west coasts of the islands [15–19].

The wave energy will be one of the greatest ocean renewable energy resources, especially in islands and archipelagos where the bathymetric auspicious the generation of important wave energy concentrations [20–23].

Ocean energy is a fairly young sector and it is still developing. Over the coming years, one of these most powerful sources, wave energy, is estimated to play an important role in reducing CO<sub>2</sub> and greenhouse gas emissions worldwide, especially in the EU. Many EU coastal countries have an important ocean energy resource, which could help reduce the emission of polluting gases from the energy system and create new

jobs. Currently in the Europe a wave energy resource has been identified in the range of 1000–1500 TWh [6,18,24,25].

The EREC (European Renewable Energy Council) considers that the marine energies, in particular wave energy, will be an important key in the goals of the European energetics strategy as it is relevant to the Directive 2009/28/EC on renewable energy. The EU has committed to reducing its polluting gas emissions by around 80–95% by 2050 [6,25–27].

The wave energy sector demands attention respect to other coastal energy technologies, for example offshore wind energy, and there are many steps in this direction [28]. Stratigaki [29] discuss one of the most important project about wave energy in Europe, the WECANet (Wave Energy Converter Array Network) European COST Action ([www.wecanet.eu](http://www.wecanet.eu), accessed on 30 August 2021). The project is supported by the European COST Association (COST stands for “European cooperation in science and technology”) and was introduced in 2018. WECANet is a consortium of professionals from 30 European member countries and United States of America. The aim of this project is to create a solid network platform focused on current challenges, identifying barriers and helping the development of wave energy research and industry.

Numerous studies and assessments about the wave energy potential have been implemented in the Macaronsian region, included the Canary Islands. On the one hand, the computer third-generation (3G) wind-wave models, WAVE Modelling (WAM) and Simulating WAVES Nearshore (SWAN) [15,17,30–33], has been used widely as an essential tool for the development of these studies. On the other hand, other numerical systems to wave forecasting in the western Atlantic Ocean based on soft computing techniques have also been used [6,34].

As general knowledge into the renewable energy industry, wave power converters (WECs) designs have not been developed for being used on a commercial scale. Moreover, an extensive number of WECs demonstration prototypes have been carried out in the EU, almost large-scale prototypes, but they ran into technical or financial problems. Despite the difficulties, the wave sector is not stopped by the setbacks and continues growing with the economic help of European governments up to the time when a competitive commercial prototype is achieved [29,35,36].

In addition, an important part in the progress and expansion of RE based on waves is the prediction of the behavior of any Wave Power Converters (WECs) based in their power matrix, especially in island regions with high wave potentials, external fuel dependency and isolated electricity systems. For that motive, the main purpose of this study is to determine the behavior of the Monte Carlo simulation to predict the energy generated from different Waves Energy Converters (WECs) in the Canary Islands, in order to establish the advantages entailed by the use of this mathematical method, in the prediction of the possible wave energy generated from a WEC. The models were carry out with the dataset from Gran Canaria buoy (2442). This buoy belongs to network buoys of the Spain’s State Ports and covers a dataset period from 1997 to 2019.

Monte Carlo method is a simulation that relies on recurrent random sampling and statistical analysis to obtain numerical results. The essential concept is to use randomness in the experiments, for which the particular result is not acknowledged in advance [37]. The mathematical simulation model can be used in many fields of engineering such as, energy model simulation [38,39], renewable energy generation, prediction and economic analysis (Wind, Photovoltaic, Wave Energy, etc.) [40–49]. The computational simulation is really useful in ocean industry too, being used in different studies such as, marine and ships structures [50–53], breakwater analysis [54], offshore wind turbine [55], maintenance operations of Wave Energy Farm [56], etc.

Other applications in the maritime field can be seen in the proposition of a new ships route decision-making strategy [57,58], reducing the accident risk in marine transportation [59], ships engine emission control [60], offshore transportation [61], ship fire consequence, etc. [62].

Some research area conditions such as regulatory frameworks, environmental impacts, social dimension, fishing activity areas, protected areas, maritime routes, military zones, bathymetry, submarine cables, pipeline protection areas, have not been considered in this study.

The goal of this paper is intended to predicting the energy transformation capability, based on historic wave data and considering the random nature of this behavior through a combination of bivariate Weibull distributions and Monte Carlo Method.

This work is structured in eight sections. After the introduction, the wave data sources from the buoy and the WECs selected for the study are shown in the section two and three. The fourth and fifth sections display the general modeling procedure of the Weibull distribution. Monte Carlo simulation of the power conversion are shown in section six. Finally, the validation the proposed model and conclusions of the whole research are given in the sections seven and eight, respectively.

## 2. Data Sources

Currently in the Canary Islands there are only five buoys that provide data on the sea waves in real time, two deep waters buoys and three nearshore buoys. The deep waters buoys are: Gran Canaria buoy (2442) at a mooring depth of 780 m, Tenerife South buoy (2446) with mooring depth of 710 m. The nearshore buoys are: Granadilla buoy (7401), 20 m depth, Santa Cruz Buoy (1421) at a mooring depth of 56 m and, Las Palmas East buoy (1414), at a depth of 30 m [63].

Data from the Gran Canaria buoy (2442) was taken to predict the energy generated from different WECs with Monte Carlo simulation in this study, because it was the buoy with the best position compared to the other buoys. It is possible to carry out this statement because the north and west of the Canary Islands are the most energetic maritime zone, due to the influence of the trade winds. Buoy 2442 has another advantage, it is the least affected by the shadow of the islands. The buoy is placed in the Northwest of Canary Islands, located at 28.20° N and 15.78° W. The geographic location of the buoy is displayed in Figure 1 [6,15,63].

The Gran Canaria buoy belongs to the deep water buoys network of the State ports of the government in Spain. This buoy is mooring at more than 200 m of deep waters. Note that, the buoy 2442 is not affected by refraction or shoaling due to the lack of continental shelf of the Canary Archipelago [6,15,63].

The data set used covers a historical period of 22 years, from 1997 to 2019, when the Gran Canaria buoy was removed to harbor for maintenance. The whole dataset was divided into a training set, which comprises data corresponding from 1997 up to year 2016, and a validation set, including data from year 2017 to year 2019.

The measurements of variables as, mean peak period,  $T$ , and wave significant spectral height,  $H$ , were carried out every three hours in the Gran Canaria buoy. The measurement accuracy was  $\pm 0.05$  s for  $T$  and  $\pm 0.05$  m for  $H$  [63]. This study has only been possible thanks to the collaboration received from the Harbors of the State of Spain, which provided the entire data set.

## 3. WECs Analyzed

The combination of wave energy systems with other renewable energies systems is particularly interesting for isolated electricity systems, which in many instances are totally isolated from continental electricity systems [64].

A retrospective of the wave energy industry shows an extensive variety of WECs concepts in development in dissimilar countries around the world [64,65]. Ahamed, McKee and Howard [65] showed that until 2019 there were more than one hundred wave energy experimental projects. All these projects have been installed and tested in dissimilar countries around the world, for example, USA, Australia, China and New Zealand. In Europe the counties involved in waves projects are Sweden, Portugal, Italy, Norway, France, Spain and UK [65,66].

Selecting the optimal deployment places involves previously feasibility studies and mathematical simulations to support the decision [67,68]. In this work, the Monte Carlo Method has been used to determine the behavior in deep water near to Canary of different tested WECs prototypes.

The number of devices considered on work are three: Pelamis (750 kW), Wave Dragon (7000 kW) and Aqua Buoy (250 kW), with different dimensions and power take off (PTO). The operating principle used for the wave energy transformation systems to change the sea wave oscillating motion into electrical energy are two, the hydraulic motor in the Pelamis case and hydro turbine, in the cases of Wave Dragon and Aqua Buoy [69–72].

The power output of any WECs in different sea states, taking into account the mean peak period,  $T$ , and the significant spectral height of the waves,  $H$ , are called power matrices. Figure 2 shows the power matrices used in the research. The sea conditions are classified into bins ( $\Delta H \times \Delta T$ ) of 0.5 m  $\times$  1.0 s, for Aqua Buoy converter; of 1.0 m  $\times$  1.0 s, for Wave Dragon converter; and of 1.0 m  $\times$  0.5 s, for Pelamis converter [66,72].

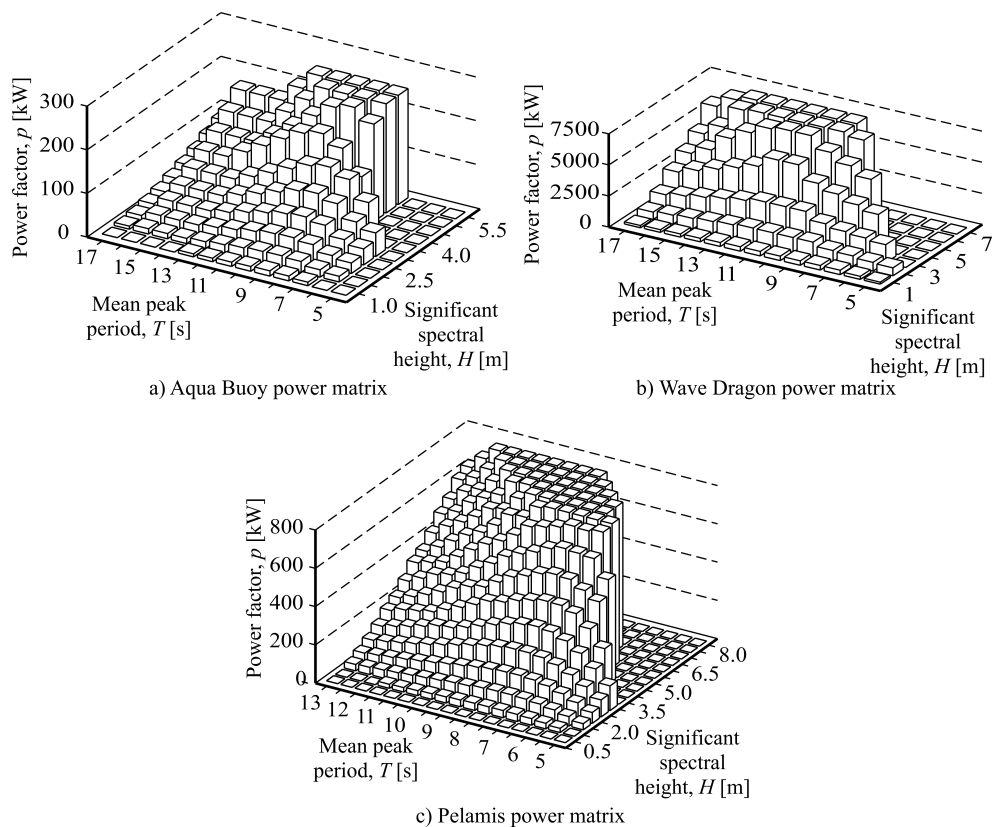


Figure 2. Power matrices for the studied WECs.

#### 4. Bivariate Weibull Distribution Fitting

For describing the stochastic behavior of the wave, given by the numerical values of the significant spectral height,  $H$ , and the mean peak period,  $T$ , a bivariate Weibull probability distribution function is fitted:

$$f(H, T) = \frac{k_1 k_2 \left(\frac{H}{c_1}\right)^{k_1-1} \left(\frac{T}{c_2}\right)^{k_2-1}}{c_1 c_2 (1 - c_{12}^2)} \times \dots \times \exp \left[ -\frac{\left(\frac{H}{c_1}\right)^{k_1} + \left(\frac{T}{c_2}\right)^{k_2}}{1 - c_{12}^2} \right] B_0 \left[ \frac{2c_{12} \left(\frac{H}{c_1}\right)^{\frac{k_1}{2}} \left(\frac{T}{c_2}\right)^{\frac{k_2}{2}}}{1 - c_{12}^2} \right]; \quad (1)$$

where  $c_1, k_1, c_2, k_2,$  and  $c_{12}$  are the distribution parameters, and  $B_0$  is the zero-order Bessel function. The corresponding parameters are obtained, through the Simultaneous Maximum Likelihood Estimate method [30,63,73,74], for each week in the year. Points in Figure 3 show the obtained values for each week, of the training set, from 1997 up to year 2016.

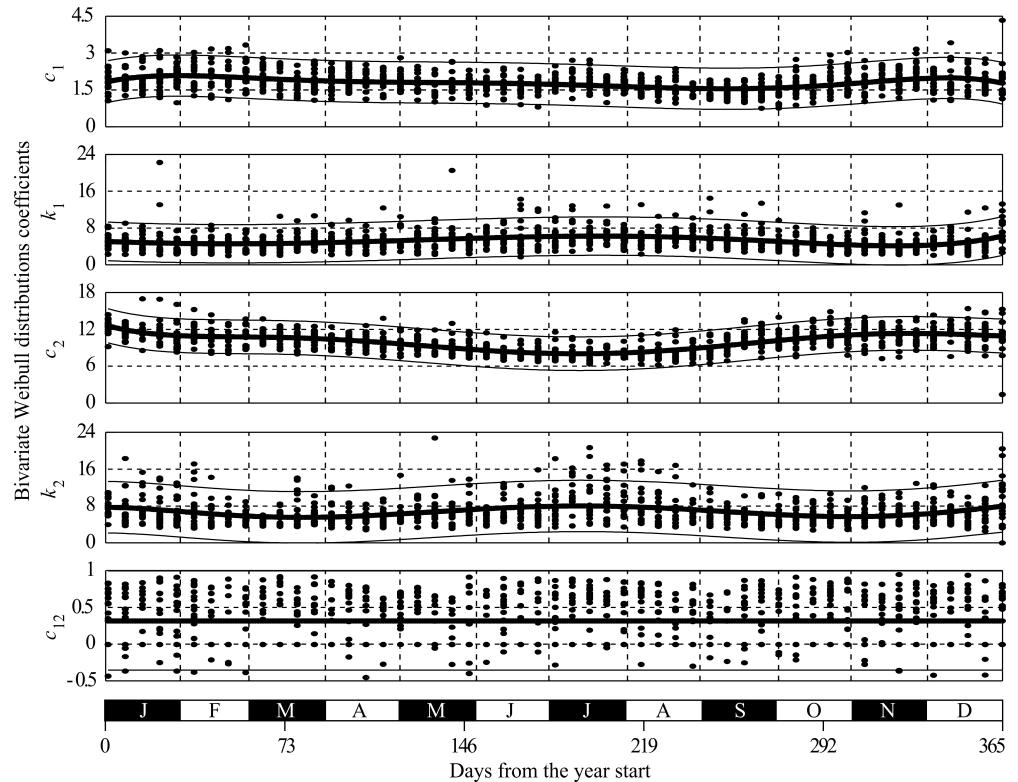


Figure 3. Bivariate Weibull coefficients of the fitted distributions.

As can be seen, all the coefficient values move around certain average. Coefficients  $c_1$  and  $c_2$ , which represents the values of significant spectral height and mean peak period, respectively, where the maximum value of probability distribution is reached, show a noticeable season variability, with higher values from October to March. Seasonal variations of coefficients  $k_1$  and  $k_2$ , which determine the shape of the probability distributions, show a light increment from May to September. Finally, it should be also noted that coefficient  $c_{12}$  does not evidence seasonal variations, indicating no changes in the interaction between significant spectral height and mean peak period.

### 5. Bivariate Weibull Coefficient Models

In order to calculate the parameters of the bivariate Weibull coefficients for each day computed from the year start,  $d$ , data from 1997 to 2016 were used. The relationship was expressed by a sixth-order polynomial equations, in the form:

$$c = \beta_6 d^6 + \dots + \beta_2 d^2 + \beta_1 d + \beta_0. \tag{2}$$

Coefficients for these models,  $\beta_6, \dots, \beta_2, \beta_1, \beta_0$ , were obtained though stepwise least square method, with backward elimination where the model starts with all the involved variables followed by an iterative deletion of the less statistically significant variable. The process is repeated until no further variable can be deleted without a statistically non-significant loss of fit. Equations used for fitting the models and obtaining the corresponding standard deviation are shown in Appendix A.

Obtained models were summarized in Table 1. As can be seen, all the probability associated with the Fisher test,  $p(F)$ , in the analysis of variance (ANOVA), are lower than 0.01, meaning that there is a statistically significant relationship between the variables,

at the 99% confidence level. The maximum values of the probability associated to the corresponding *t*-Student tests, show that all the coefficients kept in the models were statistically significant at 99% confidence level. Finally, the values of coefficient of determination ( $R^2$ ) and mean absolute error (MAE), indicate that the models as fitted explain only a low percent of the variability in the coefficients. It must be pointed out that a low  $R^2$  value does not automatically imply a bad model, especially for fields of study having an inherently greater amount of unexplainable variation (such climate phenomena [75,76]). In these cases, models can be accepted even with a low  $R^2$ , given that independent variables are statistically significant. However, the high variability in the obtained models is the main reason for using the Monte Carlo method, which allows us to evaluate the random behavior of the modeled variables.

**Table 1.** Main regression models statistics.

Model	$R^2$	MAE	$p(F)$	$\max(p(t))$
$c_1$	0.121	0.34	$\approx 0$	$1.20 \times 10^{-3}$
$k_1$	0.092	1.54	$\approx 0$	$4.78 \times 10^{-3}$
$c_2$	0.433	1.04	$\approx 0$	$2.60 \times 10^{-6}$
$k_2$	0.079	2.10	$3.00 \times 10^{-9}$	$1.62 \times 10^{-4}$
$c_{12}$	$\approx 0$	0.31	$\approx 0$	$\approx 0$

Figure 3 shows the predicted values (thick lines) and the 95% confidence intervals (thin lines). It can be noted that the predicted values of  $c_1$  (which determines the value of significant spectral height were the probability function reaches its maximum) moves from 1.5 to 2.1, with highest values in winter (November–February) and lowest values at the end of the summer (August–September).

The predicted values of  $k_1$  range from 4.1 to 6.3, which determines a bell-shaped probability function, on the significant spectral height dimension. This model reaches its maximum in June–July and minima in February and November.

The values of  $c_2$  determines the value of the mean peak period where the probability function achieves its maximum. The corresponding predicted values of  $c_2$  range from 8.1 to 12.6. The highest values for this coefficient take place in winter (November to February), while its lowest values, in summer (June and July).

The predicted values of  $k_2$  range from 5.5 to 8.8. Two minima can be observed, for these predicted values, corresponding to March–April and October–November, and two maxima, in December–January and June–July.

The last model ( $c_{12}$ ) is a special case, because all the terms, except the constant, are statistically non-significant. Consequently, the equation is just a constant, meaning that there is not a significant variation of  $c_{12}$  with the time and all the observed variability has a random nature.

All the fitted models, and the corresponding standard deviations of their residuals, are shown in Appendix B.

## 6. Monte Carlo Simulation of the Power Conversion

### 6.1. Random Values Generation

In order to perform the Monte Carlo based simulations, random generators should be defined for each bivariate Weibull distribution coefficient. These generators consist on normally distributed random numbers, with means and standard deviations as computed, in the previous subsection, for each coefficient. This can be formalized through the equation:

$$\hat{c} = \mathcal{N}[\mu(c), \sigma(c)]; \tag{3}$$

where  $\hat{c}$  is a random value of coefficient  $c$ ,  $\mathcal{N}(\bullet, \bullet)$  is the normally distributed random number, and  $\mu(c)$  and  $\sigma(c)$  are the estimated mean and standard deviation of coefficient  $c$ .

Figure 4 shows thirty random generated values, for each bivariate Weibull, in the whole interval of days of the year. As can be noted, there is a good matching between the observed (see Figure 3) and predicted values for all the coefficients.

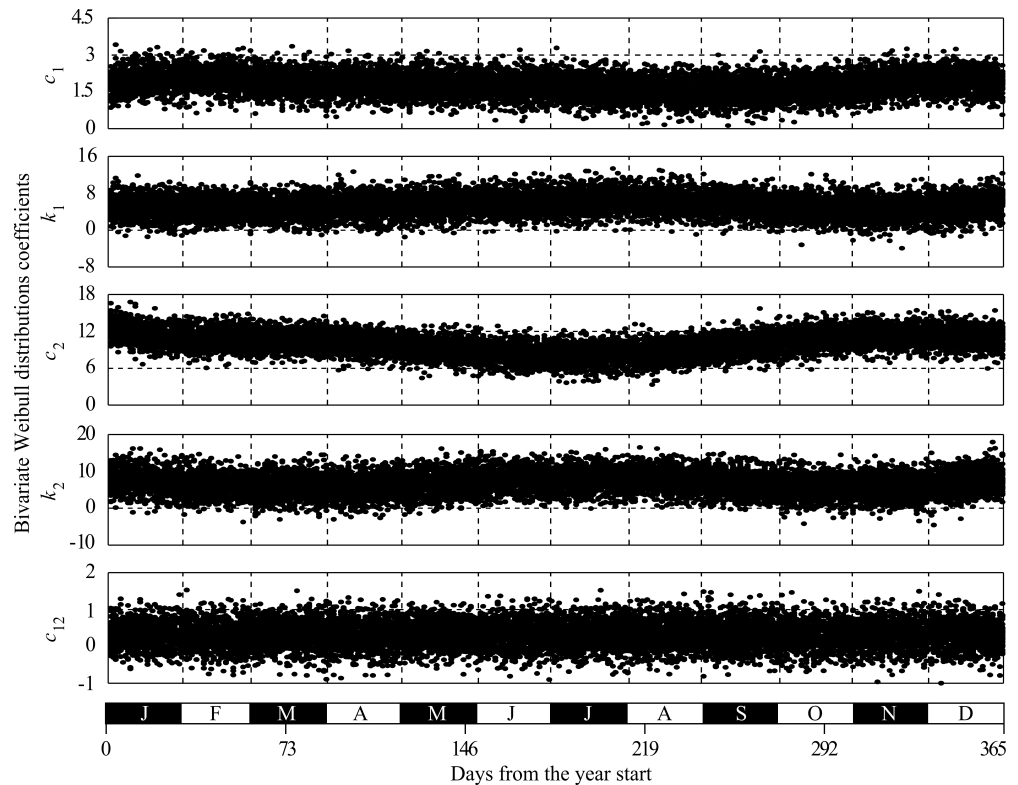


Figure 4. Randomly generated values of bivariate Weibull distribution coefficients.

6.2. Power Conversion Computing

The power conversion capabilities of the analyzed point, was studied with three different devices: Aqua Buoy, Wave Dragon and Pelamis. Each of them has the corresponding power matrix, which are shown in Figure 2.

With every randomly generated set of bivariate Weibull coefficients, the cumulative probability, in each interval of the matrix ( $H_l \leq H \leq H_u, T_l \leq T \leq T_u$ ), is determined, by the equation:

$$p|_{H_l \leq H \leq H_u, T_l \leq T \leq T_u} = \int_{H_l}^{H_u} \int_{T_l}^{T_u} f(H, T) dHdT; \tag{4}$$

where  $f(H, T)$  is the Weibull probability distribution function, given by Equation (1). This probability is numerically computed, by using the fifth order Gauss–Legendre quadrature for double integrals:

$$p|_{H_l \leq H \leq H_u, T_l \leq T \leq T_u} = \frac{(H_u - H_l)(T_u - T_l)}{4} \sum_{i=1}^5 \sum_{j=1}^5 w_i w_j f(H_i, T_j); \tag{5}$$

where  $H_i$  and  $T_j$  can be computed by the expressions:

$$H_i = \frac{H_u + H_l}{2} + \frac{H_u - H_l}{2} \xi_i; \tag{6a}$$

$$T_j = \frac{T_u + T_l}{2} + \frac{T_u - T_l}{2} \xi_j; \tag{6b}$$

and  $w_i$  and  $\xi_i$  are the corresponding weights and evaluation points (see Table 2) [77].



**Table 2.** Gauss–Legendre weights and positions.

$i$	$w_i$	$\zeta_i$
1	0.236927	−0.906180
2	0.478629	−0.538469
3	0.568889	0.000000
4	0.478629	0.538469
5	0.236927	0.906180

The total converted power,  $P$ , for each device is then computed through the expression:

$$P = \sum_{i=1}^m \sum_{j=1}^n p |_{H_j^i \leq H \leq H_u^i, T_j^i \leq T \leq T_u^i} \phi |_{H_j^i \leq H \leq H_u^i, T_j^i \leq T \leq T_u^i} \quad (7)$$

where  $m$  and  $n$  are the intervals for significant spectral height and mean peak period;  $\phi$  represents the conversion power for the considered interval and  $[H_j^i, H_u^i]$  and  $[T_j^i, T_u^i]$  are these intervals. Figure 5 shows the graphical representation of the computed converted power, for the 30 random bivariate Weibull distributions, through the year, and the corresponding mean value and 90% prediction interval.

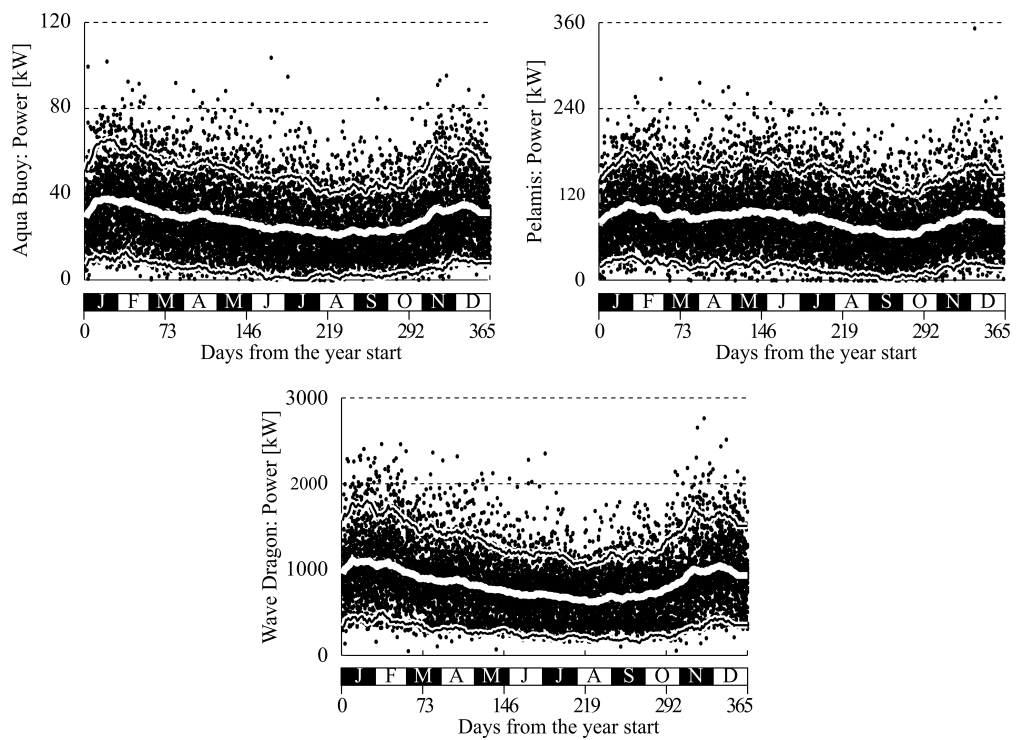


**Figure 5.** Random points, mean values and 90% prediction intervals for converted power.

As it can be appreciated in Figure 5, the conversion of sea wave oscillating motion into electrical energy, is not excessively high in the selected point for the study, if the nominal power of the Pelamis (750 kW), Wave Dragon (7000 kW) and Aqua Buoy (250 kW) WECs are taken into consideration.

**7. Validation**

In order to validate the proposed model, the prediction interval for each month was computed for each month of the year. The obtained outcomes were compared with the actual computed values for years from 2017 to 2019 (see Figure 6).

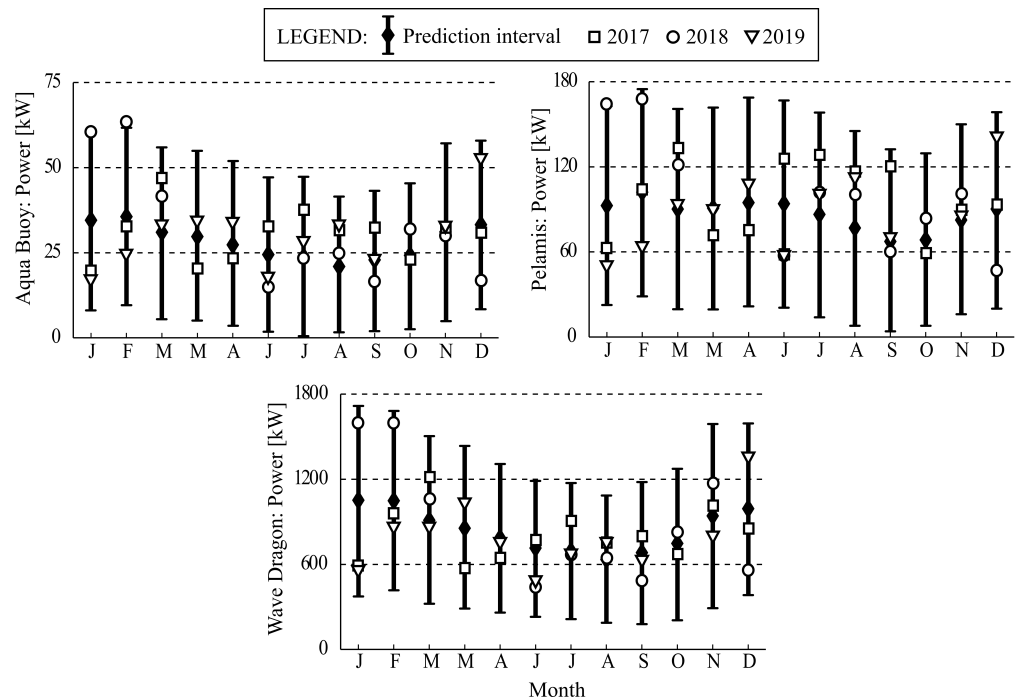


Figure 6. Predicted and observed monthly power.

It is worth mentioning that the entire observed values fell into the predicted intervals, except those corresponding to January and February 2018 in the Pelamis and Aqua Buoy converters, respectively. However, these values are very close to the upper limits.

An interesting issue arises from comparing the performance (i.e., the ration between the actual and nominal converted energy) of the three evaluated converters. In spite of the remarkable contrasts in the amount of converted energy, there are not noticeable differences in their performances. As can be seen (Figure 7), the average converted power ranges from 6% to 18%, while the maximum converted power ranges from 12% to 30%. The cause of this similarity is the divergence between the maximum probability values for the waves significant spectral wave and mean peak period (from 1 to 3 m and from 6 to 15 s, respectively), and the values where the maximum energy conversion takes place for the three converters (see Figure 2).

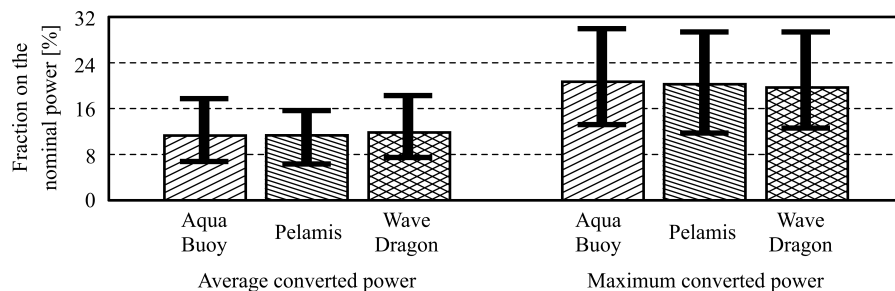


Figure 7. Performance comparison of the evaluated converters.

### 8. Conclusions

The transformation of sea waves oscillating motion into electrical energy, signifies a complex and expensive challenge. Currently there are abundant WECs concepts, but there is no consensus about a unique design approach. It might be caused by the high cost of the obtained kilowatts.

This research presents a mathematical simulation based in Monte Carlo Method, to predict the energy generated from different WECs in Canary Islands. The model was

implemented and validated with dataset from Gran Canaria deep waters buoy (2442), which belongs to the network buoys of Spain's State Ports.

In the bivariate Weibull distribution fitting used in the study, the distribution parameters  $c_1$ ,  $k_1$ ,  $c_2$ ,  $k_2$ , and  $c_{12}$ , moves around certain average, a season variability can also be detected, in  $c_1$  and  $c_2$  parameters.

In the polynomial regressions used to model the relationship between the coefficients values and day number, it is possible to see that in the regression model for the coefficients  $c_1$ ,  $k_1$ ,  $c_2$  and  $k_2$ , the probability value of the ANOVA table was lower than 0.01. This means that there is a statistically significant relationship between the variables at the 99% confidence level. With respect to  $c_{12}$ , it is possible to affirm that there not a significant variation with the time of the coefficient and all the observed variability has a random nature. It should be recalled that the small  $R^2$  values obtained in the study does not imply a wrong model, particularly for very noisy models, such as those based on climatic observations. Before calculating the wave power conversion of each WEC, it is necessary to perform the Monte Carlo-based simulations for each bivariate Weibull distribution coefficient, which simulation shows a good matching between the observed and predicted values for all the coefficients.

The power conversion capabilities or power take off (PTO) of the study devices, Pelamis, Wave Dragon and Aqua Buoy on the analyzed point (buoy 2442) was calculated with the power matrices of each one. The transformation of ocean wave oscillating motion into electrical energy, is not so high in the selected point for the study, taking into consideration the nominal power of the WECs. This results do not differ from the quality of the model based in the Monte Carlo Method, being demonstrated its effectiveness in the validation process.

The proposed approach has two main advantages. In the first place, considering the variability in the wave behavior allows to predict not only the expected converted energy but also its actual confidence interval. This plays a key role in the design of power systems where minimum delivered energy should be taken into account. In the second place, this methodology offers a model for the wave behavior, based on the bivariate Weibull distribution, and uses this model for simulating the performance of a given wave energy converter. Separating both steps, it is possible to evaluate new converters without fitting a new model, which cannot be done through other approaches, such as time series-based modeling of the converted power, directly evaluated from the raw measured wave data.

The model developed in this study could be an effective tool to calculate effectively and precisely the PTO of different WECs at any position in deep ocean waters, preferably on isolated islands of the Atlantic Ocean. The model will be useful in forecasting renewable energies, this energy can be introduced into the electrical network, used directly in desalination plants or in combination with other kind of renewable energies.

**Author Contributions:** Conceptualization, D.A.; methodology, D.A.; software, R.Q.; validation, R.Q.; formal analysis, G.N.M.; investigation, D.A.; resources, F.S.L.; data curation, G.N.M.; writing—original draft preparation, G.N.M.; writing—review and editing, F.S.L.; visualization, R.Q.; supervision, G.N.M.; project administration, D.A.; funding acquisition, F.S.L. All authors have read and agreed to the published version of the manuscript.

**Funding:** This research has been co-funded by FEDER funds, INTERREGMAC 2014–2020 Programme of the European Union, within the DESAL+ Project (MAC/1.1a/094) and the E5DES project (MAC2/1.1a/309).

**Institutional Review Board Statement:** Not applicable.

**Informed Consent Statement:** Not applicable.

**Data Availability Statement:** Not applicable.

**Acknowledgments:** The authors would like to thank Puertos del Estado (Spain's State Ports) for having provided the datasets of the buoys used in the study and the Technological Institute of the Canary Island (ITC) for the given support.

**Conflicts of Interest:** The authors declare no conflict of interest. The funders had no role in the design of the study; in the collection, analyses, or interpretation of data; in the writing of the manuscript, or in the decision to publish the results.

**Appendix A. General Modeling Procedure**

For modeling the relationship between the coefficients values and day number, measured from the year start,  $d$ , polynomial regressions, in the form:

$$c = \beta_6 d^6 + \dots + \beta_2 d^2 + \beta_1 d + \beta_0; \tag{A1}$$

were fitted. Coefficients  $\beta = \{\beta_6, \dots, \beta_2, \beta_1, \beta_0\}^T$  were obtained by using the expression:

$$\beta = (D^T D)^{-1} D^T c; \tag{A2}$$

where the days (independent variable) values, of the training dataset, are arranged into the matrix,

$$D = \{d_1, d_2, \dots, d_n\}^T; \tag{A3}$$

being:

$$d_i = \{d_i^6, \dots, d_i^2, d_i, 1\}^T; \tag{A4}$$

the vector of the powers for the  $i$ -th day value in the dataset, while the corresponding coefficients (dependent variables) values are arranged into the vector:

$$c = \{c_1, c_2, \dots, c_n\}^T. \tag{A5}$$

For a given day vector:

$$\tilde{d} = \{\tilde{d}^6, \dots, \tilde{d}^2, \tilde{d}, 1\}^T; \tag{A6}$$

(either included in the training dataset or not), the mean value of the corresponding coefficient prediction,  $\mu(c)$  can be determined through the equation:

$$\mu(c) = \tilde{d}^T \beta. \tag{A7}$$

Meanwhile, the standard deviation for this prediction,  $\sigma(c)$ , can be estimated by the expression:

$$\sigma(c) = \bar{\sigma} \sqrt{\tilde{d}^T (D^T D)^{-1} \tilde{d} + 1}; \tag{A8}$$

where:

$$\bar{\sigma} = \frac{e^T e}{n - p}; \tag{A9}$$

is the standard deviation of the residuals:

$$e = c - D\beta; \tag{A10}$$

and  $n$  and  $p$  are, respectively, the number of training dataset samples and the number of considered model coefficients.

**Appendix B. Regression Models Equations**

*Appendix B.1. Regression Model for Coefficient  $c_1$*

$$\begin{aligned} \mu(c_1) = & -7.95262696 \times 10^{-14} d^6 + 8.48197198 \times 10^{-11} d^5 - 3.42526309 \times 10^{-8} d^4 \dots \\ & \dots + 6.57254327 \times 10^{-6} d^3 - 6.09286438 \times 10^{-4} d^2 + 2.19854430 \times 10^{-2} d \dots \\ & \dots + 1.81818137. \end{aligned} \tag{A11}$$

$$\begin{aligned} \sigma(c_1) = & (3.26762710 \times 10^{-28}d^{12} - 7.18755785 \times 10^{-25}d^{11} + 6.96997361 \times 10^{-22}d^{10} \dots \\ & \dots - 3.36260928 \times 10^{-19}d^9 + 1.41687872 \times 10^{-17}d^8 - 3.43986618 \times 10^{-14}d^7 \dots \\ & \dots + 5.70244909 \times 10^{-12}d^6 - 6.43188002 \times 10^{-10}d^5 + 4.83054479 \times 10^{-8}d^4 \dots \\ & \dots - 2.31519716 \times 10^{-6}d^3 + 6.59426911 \times 10^{-5}d^2 - 9.97657046 \times 10^{-4}d \dots \\ & \dots + 1.8967827)^{1/2}. \end{aligned} \quad (A12)$$

Appendix B.2. Regression Model for Coefficient  $k_1$

$$\begin{aligned} \mu(k_1) = & 3.74524820 \times 10^{-14}d^6 - 1.65092509 \times 10^{-11}d^5 + 2.02313104 \times 10^{-4}d^2 \dots \\ & \dots - 2.03090419d + 5.15610950. \end{aligned} \quad (A13)$$

$$\begin{aligned} \sigma(k_1) = & (2.50205143 \times 10^{-29}d^{12} - 2.25211476 \times 10^{-26}d^{11} + 5.10345445 \times 10^{-24}d^{10} \dots \\ & + 3.64447234 \times 10^{-19}d^8 - 2.26313621 \times 10^{-16}d^7 + 2.80072483 \times 10^{-14}d^6 \dots \\ & - 6.92433043 \times 10^{-13}d^5 + 1.65426604 \times 10^{-9}d^4 - 5.65252131 \times 10^{-7}d^3 \dots \\ & \dots + 6.84889839 \times 10^{-5}d^2 - 3.49129949 \times 10^{-3}d + 4.54222458)^{1/2}. \end{aligned} \quad (A14)$$

Appendix B.3. Regression Model for Coefficient  $c_2$

$$\begin{aligned} \mu(c_2) = & 2.78608215 \times 10^{-13}d^6 - 3.35020170 \times 10^{-10}d^5 + 1.48761913 \times 10^{-7}d^4 \dots \\ & \dots - 2.97827269 \times 10^{-5}d^3 + 2.69987876 \times 10^{-3}d^2 - 0.115033275d + 12.7051253. \end{aligned} \quad (A15)$$

$$\begin{aligned} \sigma(c_2) = & (3.46946634 \times 10^{-27}d^{12} - 7.63152872 \times 10^{-24}d^{11} + 7.40050445 \times 10^{-21}d^{10} \dots \\ & \dots - 4.16324882 \times 10^{-18}d^9 + 1.50439841 \times 10^{-15}d^8 - 3.65234453 \times 10^{-13}d^7 \dots \\ & \dots + 6.05468574 \times 10^{-11}d^6 - 6.82917316 \times 10^{-9}d^5 + 5.12892446 \times 10^{-7}d^4 \dots \\ & \dots - 2.45820542 \times 10^{-5}d^3 + 7.00159292 \times 10^{-4}d^2 - 0.0105928169d + 2.00852604)^{1/2}. \end{aligned} \quad (A16)$$

Appendix B.4. Regression Model for Coefficient  $k_2$

$$\begin{aligned} \mu(k_2) = & -2.93514162 \times 10^{-13}d^6 + 3.42377365 \times 10^{-10}d^5 - 1.4370226 \times 10^{-7}d^4 \dots \\ & \dots + 2.55866129 \times 10^{-5}d^3 - 0.00163200606d^2 + 7.74516819. \end{aligned} \quad (A17)$$

$$\begin{aligned} \sigma(k_2) = & 6.00329821 \times 10^{-27}d^{12} - 1.21221006 \times 10^{-23}d^{11} + 1.05985695 \times 10^{-20}d^{10} \dots \\ & \dots - 5.24463883 \times 10^{-18}d^9 + 1.60906763 \times 10^{-15}d^8 - 3.14249078 \times 10^{-13}d^7 \dots \\ & \dots + 3.82842154 \times 10^{-11}d^6 - 2.65414825 \times 10^{-9}d^5 + 7.22037679 \times 10^{-8}d^4 \dots \\ & \dots + 1.97789189 \times 10^{-6}d^3 - 0.00013677311d^2 + 8.14821077. \end{aligned} \quad (A18)$$

Appendix B.5. Regression Model for Coefficient  $c_{12}$

$$\mu(c_{12}) = 0.32245646. \quad (A19)$$

$$\sigma(c_{12}) = 0.11637072. \quad (A20)$$

## References

1. Fernández, J.M. Spain in the European Union. 2016. Available online: [http://www.cvce.eu/obj/spain\\_in\\_the\\_european\\_union-en-7d6933cb-1a23-468c-bb15-93c2cf18c91f.html](http://www.cvce.eu/obj/spain_in_the_european_union-en-7d6933cb-1a23-468c-bb15-93c2cf18c91f.html) (accessed on 6 July 2020).
2. European Commission. The Outermost Regions of the European Union: Towards a Partnership for Smart, Sustainable and Inclusive Growth. 2012. Available online: <https://eur-lex.europa.eu/LexUriServ/LexUriServ.do?uri=COM%3A2012%3A0287%3AFIN%3AEN%3Apdf> (accessed on 6 July 2020).
3. Schallenberg, J.; Veza, J.M.; Blanco-Marigorta, A. Energy efficiency and desalination in the Canary Islands. *Renew. Sustain. Energy Rev.* **2014**, *40*, 741–748. [[CrossRef](#)]
4. Gils, H.C.; Simon, S. Carbon neutral archipelago-100% renewable energy supply for the Canary Islands. *Appl. Energy* **2017**, *188*, 342–355. [[CrossRef](#)]
5. González, A.; Pérez, J.C.; Díaz, J.; Expósito, F. Future projections of wind resource in a mountainous archipelago, Canary Islands. *Renew. Energy* **2017**, *104*, 120–128. [[CrossRef](#)]
6. Ávila, D.; Marichal, G.N.; Padrón, I.; Quiza, R.; Hernández, A. Forecasting of wave energy in Canary Islands based on artificial intelligence. *Appl. Ocean Res.* **2020**, *101*, 102–189. [[CrossRef](#)]
7. Sundseth, K. *Natura 2000 in the Macaronesian Region*; European Communities: 2009; Available online: <https://ec.europa.eu/environment/nature/info/pubs/docs/biogeos/Macaronesian.pdf> (accessed on 25 August 2021).
8. Cropper, T.E.; Hanna, E. An analysis of the climate of Macaronesia, 1865–2012. *Int. J. Climatol.* **2014**, *34*, 604–622. [[CrossRef](#)]
9. Meco, J.; Koppers, A.A.; Miggins, D.P.; Lomoschitz, A.; Betancort, J.F. The Canary record of the evolution of the North Atlantic Pliocene: New <sup>40</sup>Ar/<sup>39</sup>Ar ages and some notable palaeontological evidence. *Palaeogeogr. Palaeoclimatol. Palaeoecol.* **2015**, *435*, 53–69. [[CrossRef](#)]
10. Padrón, I.; Ávila, D.; Marichal, G.N.; Rodríguez, J.A. Assessment of hybrid renewable energy systems to supplied energy to autonomous desalination systems in two islands of the Canary Archipelago. *Renew. Sustain. Energy Rev.* **2019**, *101*, 221–230. [[CrossRef](#)]
11. Fontán-Bouzas, Á.; Alcántara-Carrió, J.; Albarracín, S.; Baptista, P.; Silva, P.A.; Portz, L.; Manzolli, R.P. Multiannual shore morphodynamics of a cusped foreland: Maspalomas (Gran Canaria, Canary Islands). *J. Mar. Sci. Eng.* **2019**, *7*, 416. [[CrossRef](#)]
12. ISTAC (Canarian Statistic Institute). 2020. Available online: <https://www.statcan.gc.ca/eng/start> (accessed on 15 July 2020).
13. Electrical Network of Spain. The Importance of a Connected Electrical Energy [El Valor de una Energía Conectada]. 2016. Available online: [https://www.ree.es/sites/default/files/downloadable/diptico\\_canarias\\_2016\\_esp.pdf](https://www.ree.es/sites/default/files/downloadable/diptico_canarias_2016_esp.pdf) (accessed on 15 July 2020).
14. Frydrychowicz-Jastrzebska, G. El Hierro renewable energy hybrid system: A tough compromise. *Energies* **2018**, *11*, 2812. [[CrossRef](#)]
15. Gonçalves, M.; Martinho, P.; Guedes, C. Assessment of wave energy in the Canary Islands. *Renew. Energy* **2014**, *68*, 774–784. [[CrossRef](#)]
16. Fernández Prieto, L.; Rodríguez Rodríguez, G.; Schallenberg Rodríguez, J. Wave energy to power a desalination plant in the north of Gran Canaria Island: Wave resource, socioeconomic and environmental assessment. *J. Environ. Manag.* **2019**, *231*, 546–551. [[CrossRef](#)] [[PubMed](#)]
17. Iglesias, G.; Carballo, R. Wave resource in El Hierro: An island towards energy self-sufficiency. *Renew. Energy* **2011**, *36*, 689–698. [[CrossRef](#)]
18. Lavidas, G.; Venugopal, V.; Friedrich, D. Wave energy extraction in Scotland through an improved nearshore wave atlas. *Int. J. Mar. Energy* **2017**, *17*, 64–83. [[CrossRef](#)]
19. IDAE [Institute for the Diversification and Saving of Energy]. Wave Energy Evaluation. Technical Study. PER 2011–2020. 2011. Available online: [https://www.idae.es/uploads/documentos/documentos\\_11227\\_e13\\_olas\\_b31fcafb.pdf](https://www.idae.es/uploads/documentos/documentos_11227_e13_olas_b31fcafb.pdf) (accessed on 10 June 2020).
20. Falcão, A.F.O. Wave energy utilization: A review of the technologies. *Renew. Sustain. Energy Rev.* **2010**, *14*, 899–918. [[CrossRef](#)]
21. Rusu, E.; Guedes Soares, C. Wave energy pattern around the Madeira Islands. *Energy* **2012**, *45*, 771–785. [[CrossRef](#)]
22. Song, R.; Zhang, M.; Qian, X.; Wang, X.; Dai, Y.M.; Chen, J. A floating ocean energy conversion device and numerical study on buoy shape and performance. *J. Mar. Sci. Eng.* **2016**, *4*, 35. [[CrossRef](#)]
23. Harnois, V.; Thies, P.R.; Johanning, L. On peak mooring loads and the influence of environmental conditions for marine energy converters. *J. Mar. Sci. Eng.* **2016**, *4*, 29. [[CrossRef](#)]
24. O’Hagan, A.; Huertas, C.; O’Callaghan, J.; Greaves, D. Wave energy in Europe: Views on experiences and progress to date. *Int. J. Mar. Energy* **2016**, *14*, 180–197. [[CrossRef](#)]
25. European Commission. *Study on Lessons for Ocean Energy Development: Final Report*; Publications Office of the European Union, Luxembourg: 2017. Available online: <https://op.europa.eu/en/publication-detail/-/publication/03c9b48d-66af-11e7-b2f2-01aa75ed71a1> (accessed on 15 July 2020).
26. EREC [European Renewable Energy Council]. Mapping Renewable Energy Pathways towards 2020: EU Roadmap. 2011. Available online: [http://www.eufors.org/fileadmin/eufors/Projects/REPAP\\_2020/EREC-roadmap-V4.pdf](http://www.eufors.org/fileadmin/eufors/Projects/REPAP_2020/EREC-roadmap-V4.pdf) (accessed on 16 July 2020).
27. European Commission. Blue Energy Action Needed to Deliver on the Potential of Ocean Energy in European Seas and Oceans by 2020 and Beyond. 2014. Available online: <https://eur-lex.europa.eu/legal-content/EN/TXT/?uri=CELEX%3A52014DC0008> (accessed on 18 July 2020).

28. Trueworthy, A.; DuPont, B. The wave energy converter design process: Methods applied in industry and shortcomings of current practices. *J. Mar. Sci. Eng.* **2020**, *8*, 932. [CrossRef]
29. Stratigaki, V. WECANet: The first open Pan-European network for marine renewable energy with a focus on wave energy-COST action CA17105. *Water* **2019**, *11*, 1249. [CrossRef]
30. Barstow, S.; Mørk, G.; Mollison, D.; Cruz, J. The wave energy resource. In *Ocean Wave Energy: Current Status and Future Perspectives*; Cruz, J., Ed.; Springer: Berlin/Heidelberg, Germany, 2008; pp. 93–132.
31. Puscasu, R. Integration of artificial neural networks into operational ocean wave prediction models for fast and accurate emulation of exact nonlinear interactions. *Procedia Comput. Sci.* **2014**, *29*, 1156–1170. [CrossRef]
32. The Wamdi Group. The WAM model: A third generation ocean wave prediction model. *J. Phys. Oceanogr.* **1988**, *18*, 1775–1810. [CrossRef]
33. SWAN Team. SWAN Scientific and Technical Documentation. 2020. Available online: <http://swanmodel.sourceforge.net/download/zip/swantech.pdf> (accessed on 3 September 2020).
34. Malekmohamadi, I.; Bazargan-Lari, M.R.; Kerachian, R.; Nikoo, M.R.; Fallahnia, M. Evaluating the efficacy of SVMs, BNs, ANNs and ANFIS in wave height prediction. *Ocean Eng.* **2011**, *38*, 487–497. [CrossRef]
35. Molina, O.; Castro, F.; Harrison, R.L. Efficiency assessments for different WEC types in the Canary Islands. In *Developments in Maritime Transportation and Exploitation of Sea Resources*; Soares, G., Peña, L., Eds.; Taylor and Francis Group: London UK, 2014; pp. 879–887.
36. Babarit, A.; Hals, J.; Muliawan, M.; Kurniawan, A.; Moan, T.; Krokstad, J. Numerical benchmarking study of a selection of wave energy converters. *Renew. Energy* **2012**, *41*, 44–63. [CrossRef]
37. Raychaudhuri, S. Introduction to Monte Carlo simulation. In Proceedings of the 40th Conference on Winter Simulation, Miami, FL, USA, 7–10 December 2008; pp. 91–100.
38. Urquizo, J.; Calderón, C.; James, P. Using a local framework combining principal component regression and Monte Carlo simulation for uncertainty and sensitivity analysis of a domestic energy model in sub-city areas. *Energies* **2017**, *10*, 1986. [CrossRef]
39. Kryzia, D.; Kuta, M.; Matuszewska, D.; Olczak, P. Analysis of the potential for gas micro-cogeneration development in Poland using the Monte Carlo method. *Energies* **2020**, *13*, 3140. [CrossRef]
40. Da Silva Pereira, E.D.; Tavares Pinho, J.; Barros Galhardo, M.A.; Negrão Macêdo, W. Methodology of risk analysis by Monte Carlo method applied to power generation with renewable energy. *Renew. Energy* **2014**, *69*, 347–355. [CrossRef]
41. Caralis, G.; Diakoulaki, D.; Yang, P.; Gao, Z.; Zervos, A.; Rados, K. Profitability of wind energy investments in China using a Monte Carlo approach for the treatment of uncertainties. *Renew. Sustain. Energy Rev.* **2014**, *40*, 224–236. [CrossRef]
42. López-Ruiz, A.; Bergillos, R.J.; Ortega-Sánchez, M. The importance of wave climate forecasting on the decision-making process for nearshore wave energy exploitation. *Appl. Energy* **2016**, *182*, 191–203. [CrossRef]
43. Hrafnkelsson, B.; Oddsson, G.; Unnthorsson, R. A method for estimating annual energy production using Monte Carlo wind speed simulation. *Energies* **2016**, *9*, 286. [CrossRef]
44. Martinez-Velasco, J.A.; Guerra, G. Analysis of distribution systems with photovoltaic generation using a power flow simulator and a parallel Monte Carlo approach. *Energies* **2016**, *9*, 537. [CrossRef]
45. Hiles, C.E.; Beatty, S.J.; De Andres, A. Wave energy converter annual energy production uncertainty using simulations. *J. Mar. Sci. Eng.* **2016**, *4*, 53. [CrossRef]
46. Amirinia, G.; Kamranzad, B.; Mafi, S. Wind and wave energy potential in southern Caspian Sea using uncertainty analysis. *Energy* **2017**, *120*, 332–345. [CrossRef]
47. Liu, W.; Guo, D.; Xu, Y.; Cheng, R.; Wang, Z.; Li, Y. Reliability assessment of power systems with photovoltaic power stations based on intelligent state space reduction and pseudo-sequential Monte Carlo simulation. *Energies* **2018**, *11*, 1431. [CrossRef]
48. Wu, G.; Liu, C.; Liang, Y. Comparative study on numerical calculation of 2-d random sea surface based on fractal method and Monte Carlo method. *Water* **2020**, *12*, 1871. [CrossRef]
49. Younesian, D.; Alam, M.R. Multi-stable mechanisms for high-efficiency and broadband ocean wave energy harvesting. *Appl. Energy* **2017**, *197*, 292–302. [CrossRef]
50. Naess, A.; Gaidai, O.; Teigen, P. Extreme response prediction for nonlinear floating offshore structures by Monte Carlo simulation. *Appl. Ocean Res.* **2007**, *29*, 221–230. [CrossRef]
51. Naess, A.; Gaidai, O.; Haver, S. Efficient estimation of extreme response of drag-dominated offshore structures by Monte Carlo simulation. *Ocean Eng.* **2007**, *34*, 2188–2197. [CrossRef]
52. Bang, A.; Vanem, E.; Natvig, B. A new approach to environmental contours for ocean engineering applications based on direct Monte Carlo simulations. *Ocean Eng.* **2013**, *60*, 124–135. [CrossRef]
53. Lin, W.; Su, C. An efficient Monte-Carlo simulation for the dynamic reliability analysis of jacket platforms subjected to random wave load. *J. Mar. Sci. Eng.* **2021**, *9*, 380. [CrossRef]
54. Levent, M.; Elmar, C. Reliability analysis of a rubble mound breakwater using the theory of fuzzy random variables. *Appl. Ocean Res.* **2012**, *39*, 83–88. [CrossRef]
55. Chian, C.Y.; Zhao, Y.Q.; Lin, T.Y.; Nelson, B.; Huang, H.H. Comparative study of time-domain fatigue assessments for an offshore wind turbine jacket substructure by using conventional grid-based and Monte Carlo sampling methods. *Energies* **2018**, *11*, 3112. [CrossRef]

56. Rinaldi, G.; Thies, P.; Walker, R.; Johanning, L. On the analysis of a wave energy farm with focus on maintenance operations. *J. Mar. Sci. Eng.* **2016**, *4*, 51. [[CrossRef](#)]
57. Kim, S.W.; Jang, H.K.; Cha, Y.J.; Yu, H.S.; Lee, S.J.; Yu, D.H.; Lee, A.R.; Jin, E.J. Development of a ship route decision-making algorithm based on a real number grid method. *Appl. Ocean Res.* **2020**, *101*, 102230. [[CrossRef](#)]
58. Zhou, G.; Wang, Y.; Zhao, D.; Lin, J. Uncertainty analysis of ship model propulsion test on actual seas based on Monte Carlo method. *J. Mar. Sci. Eng.* **2020**, *8*, 398. [[CrossRef](#)]
59. Faghih-Roohi, S.; Xie, M.; Ming, K. Accident risk assessment in marine transportation via Markov modelling and Markov Chain Monte Carlo simulation. *Ocean Eng.* **2014**, *9*, 363–370. [[CrossRef](#)]
60. Kana, A.; Harrison, B. A Monte Carlo approach to the ship-centric Markov decision process for analyzing decisions over converting a containership to LNG power. *Ocean Eng.* **2017**, *130*, 40–48. [[CrossRef](#)]
61. Kim, B.; Kim, T.W. Monte Carlo simulation for offshore transportation. *Ocean Eng.* **2017**, *129*, 177–190. [[CrossRef](#)]
62. Salem, A. Use of Monte Carlo simulation to assess uncertainties in fire consequence calculation. *Ocean Eng.* **2016**, *117*, 411–430. [[CrossRef](#)]
63. Harbors of State of Spain. Waves Average. Buoy of Gran Canaria 2442 [Clima Boya de Gran Canaria, 2442]. 2017. Available online: [http://www.puertos.es/es-es/oceanografia/Paginas/portus\\_OLD.aspx](http://www.puertos.es/es-es/oceanografia/Paginas/portus_OLD.aspx) (accessed on 8 June 2020)
64. Clemente, D.; Rosa-Santos, P.; Taveira-Pinto, F. On the potential synergies and applications of wave energy converters: A review. *Renew. Sustain. Energy Rev.* **2021**, *135*, 110–162. [[CrossRef](#)]
65. Ahamed, R.; McKee, K.; Howard, I. Advancements of wave energy converters based on power take off (PTO) systems: A review. *Ocean Eng.* **2020**, *204*, 107248. [[CrossRef](#)]
66. Padrón, I.; Avila, D.; Marichal, G. Assessment of wave energy converters systems to supplied energy to desalination systems in the El Hierro Island. In Proceedings of the 3rd International Conference on Offshore Renewable Energy. (CORE 2018), Lisbon, Portugal, 8–10 October 2018.
67. Astariz, S.; Iglesias, G. Selecting optimum locations for co-located wave and wind energy farms. Part I: The co-Location feasibility index. *Energy Convers. Manag.* **2016**, *122*, 589–598. [[CrossRef](#)]
68. Astariz, S.; Iglesias, G. Selecting optimum locations for co-located wave and wind energy farms. Part II: A case study. *Energy Convers. Manag.* **2016**, *122*, 599–608. [[CrossRef](#)]
69. Weinstein, A.; Fredrikson, G.; Parks, M.J.; Neislen, K. Aqua Buoy-The offshore wave energy converter: Numerical modeling and optimization. In Proceedings of the Oceans'04 MTS/IEEE Techno-Ocean'04, Kobe, Japan, 9–12 November 2004.
70. Henderson, R. Design, simulation, and testing of a novel hydraulic power take-off system for the Pelamis wave energy converter. *Renew. Energy* **2006**, *31*, 271–283. [[CrossRef](#)]
71. Kofoed, J.; Frigaard, P.; Friis-Madsen, E.; Sørensen, H. Prototype testing of the wave energy converter Wave Dragon. *Renew. Energy* **2006**, *31*, 181–189. [[CrossRef](#)]
72. Silva, D.; Rusu, E.; Guedes, C. Evaluation of various technologies for wave energy conversion in the Portuguese nearshore. *Energies* **2013**, *6*, 1344–1364. [[CrossRef](#)]
73. Sorensen, R. *Basic Coastal Engineering*; Springer: New York, NY, USA, 2006.
74. Desouky, M.A.A.; Abdelkhalik, O. Wave prediction using wave rider position measurements and NARX network in wave energy conversion. *Appl. Ocean Res.* **2019**, *82*, 10–21. [[CrossRef](#)]
75. Oh, S.H.; Suh, K.D.; Son, S.Y.; Lee, D.Y. Performance comparison of spectral wave models based on different governing equations including wave breaking. *J. Civ. Eng.* **2009**, *13*, 75–84. [[CrossRef](#)]
76. Dominguez, J.C.; Cienfuegos, R.; Catalán, P.; Zamorano, L.; Lucero, F. Assessment of fast spectral wave transfer methodologies from deep to shallow waters in the framework of energy resource quantification in the Chilean coast. *Coast. Eng. Proc.* **2014**, *34*, 23. [[CrossRef](#)]
77. Kiusalaas, J. *Numerical Methods in Engineering with MATLAB*; Cambridge University Press: Cambridge, UK, 2005.